Environ Earth Sci (2015) 73:4313–4323
DOI 10.1007/s12665-014-3715-6

ORIGINAL ARTICLE

Establishment of chronofunctions for dark loessial soil on the central Loess Plateau based on soil chronosequences

Gang Liu · Puling Liu · Mingyi Yang · Qiong Zhang · David N. Warrington

Received: 24 November 2013 / Accepted: 15 September 2014 / Published online: 25 September 2014

Abstract The process of soil development can be studied quantitatively by analyzing the chronofunctions of soil based on its physical and chemical characteristics, which provide a basis for establishing soil development models. In this paper, the physical and chemical characteristics as well as the ^{14}C age of Holocene dark loessial soil profiles found in Luochuan and Yanchang areas on the central Loess Plateau were analyzed to establish soil chronosequences. Then, linear functions, logarithmic functions, and third-order polynomials were used to fit the soil chronosequences to establish the soil's chronofunctions, which were verified both theoretically and empirically. In the two soil profiles, third-order polynomials could best fit the age of clay (<0.002 mm), silt (0.002–0.02 mm), and sand (0.02–2 mm), and their trends reflected the characteristics of dark loessial soil layers. The changes of soil organic carbon and pH in relation to soil age could be fitted by logarithmic functions. Lastly, third-order polynomials could best fit changes in the soil's $CaCO_3$ content and Fe/Zr, K/Zr, P/Zr, Na/Zr and Mg/Zr ratios with soil age, which represented the migration processes of $CaCO_3$ and various elements in the soil.

Keywords ^{14}C · Chronofunction · Soil genesis · Dark loessial soil · Migration

G. Liu
State Key Laboratory of Simulation and Regulation of Water Cycle in River Basin, China Institute of Water Resources and Hydropower Research, Beijing 100048, People's Republic of China

G. Liu (✉) · P. Liu · M. Yang · Q. Zhang · D. N. Warrington
State Key Laboratory of Soil Erosion and Dryland Farming on the Loess Plateau, Institute of Soil and Water Conservation, Northwest A&F University, No. 26, Xinong Road, Yangling 712100, Shaanxi, People's Republic of China
e-mail: gliu@foxmail.com

G. Liu
USDA-ARS National Sedimentation Laboratory, Oxford, MI 38655, USA

Introduction

Observing the long and complex process of soil formation is extremely difficult. However, effective quantitative research on soil development can be carried out using soil chronosequences (Vreeken 1975; Bockheim 1980). A soil chronosequence refers to the changes in physical and chemical characteristics of soil with time under similar, albeit not identical, conditions of vegetation, topography, climate and soil parent material (Vincent et al. 1994; Vidic 1998). This enables a long-term study of the changing physical and chemical characteristics of a soil to be made from different soil profiles, while also translating the spatial differences between soils into temporal differences. A soil chronosequence is a good indicator of the rate and direction of soil development, and can provide valuable information for testing pedogenetic theories. In recent years, many researchers have studied soil chronosequences and have shown that soil properties are related to time by linear, power, exponential or logarithmic functions (e.g., Bockheim 1980; Birkeland 1984; Huggett 1998; Wilcke et al. 2003). These chronofunctions are useful for studying pedogenesis, and could provide a theoretical basis for the prediction of soil remediation rates as well as supporting data for establishing soil development models (Bockheim 1980; Finke and Hutson 2008). However, these basic functions are not always the best option for representing chronofunctions. Selection of soil chronofunctions needs to

conform to reality and should be based on corresponding theories (Schaetzl et al. 1994). In addition, other functions such as hyperbolic, polynomial or non-linear functions may not only better fit the data, but also help to develop new understandings about pedogenetic systems (Schaetzl et al. 1994).

The dark loessial soil profile is a well-preserved Holocene soil profile on the Loess Plateau and provides important information for the study of climatic and environmental evolution in the Holocene (Liu 1985; Tang and He 2004; Liu et al. 2013). At present, there are abundant studies on the chronosequences of dark loessial soil profiles, but studies on the chronofunctions are rare (Hu 1994; Chen et al. 1998; Tang and He 2002). In this paper, the physical and chemical characteristics as well as the ^{14}C age of Holocene dark loessial soil from Luochuan and Yanchang Counties in Shaanxi Province on the central Loess Plateau were studied. The goal of the present study was to establish chronofunctions for the dark loessial soil on the central Loess Plateau.

Materials and methods

The study area is located on the central Loess Plateau, and has a warm, semi-humid continental monsoon climate. The Loess Plateau in northwest China covers an area of 530,000 km^2; the loess deposits that cover it typically range in thickness from 30 to 80 m. The loessial soils are characterized by yellowish colors, absence of bedding, silty texture, looseness, macroporosity, and collapsibility when saturated. The Loess Plateau is conveniently divided into three zones: sandy loess in the northern part, typical loess in the middle, and clayey loess in the south (Liu 1985). The present-day vegetation in the study area is dominated by grasses and shrubs (Poaceae, Leguminosae, Labiatae, Rhamnaceae, and Compositae).

Two soil profiles were investigated. One profile was located in Luochuan County (PLC) N35°42.561′, E109°23.952′ (Fig. 1), where the annual mean temperature is 9.2 °C and the annual rainfall is 622 mm. The second profile was located in Yanchang County (PYC) N36°36.836′, E109°56.125′ (Fig. 1), where the annual mean temperature is 8.9 °C and the annual rainfall is 510 mm. The terrains of both profiles exhibit flat plateau surfaces. A 2.0 m deep profile was dug from the surface. Profile cutters were used to treat the profile so that each horizon was clearly visible. Measuring tapes were used to measure the depth of each horizon, and the characteristics of each horizon were observed, recorded and photographed. When profile samples were collected, the superficial soil was first removed to prevent the mixing of contaminated soil with the samples. Afterwards, the profile was divided from top to bottom into 20 layers; each layer was 10 cm thick. From each layer, samples of soil bulk density were collected using cutting rings. Soil samples of 500 g were collected with plastic shovels and the samples were sealed in bags and numbered before bringing back to the laboratory. In the laboratory, after air-drying and picking out visible roots and stone fragments, samples were passed through a 2 mm sieve.

The soil samples were sent to the Accelerator Mass Spectrometry Center, CAS Institute of Earth Environment. All soil samples were oven dried (60 °C) to constant weight, then ground and sieved. To extract humic acids and to date the humin fraction alone, samples were first treated with acid and alkali solutions (Mook and Streurman 1983). All pre-treated samples were combusted by sealing the sample with CuO wire in an evacuated quartz tube, and then placing the tube in a 950 °C oven for 2 h. The resulting CO_2 was purified and reduced to graphite targets for AMS using the apparatus and methods described in Vogel et al. (1987). The calibration of the ^{14}C age used the methods of Ramsey (2001) and Reimer et al. (2004). The soil samples were treated with H_2O_2 and HCl to remove organic matter, prepared with $Na_4P_2O_7$ and treated with ultrasound for 3 min before analysis.

A standardized procedure was used for operating the Malvern Mastersizer 2000 (Malvern, UK) to measure soil particle size distributions, while a portable pH meter (PHBJ-260 pH meter, Leici, China) was used to measure the pH values of the samples. Additionally, the amounts of organic carbon and carbonate–carbon were determined by a carbon analyzer using a stepped heating routine (LECO RC 412), successively measuring both carbon fractions in two replicates. The total elements, including Fe, K, Na, Mg, and Zr were determined by an energy-dispersive X-ray fluorescence (EDXRF) spectrometer system, which consisted of a miniaturized X-ray tube (30 kV, 50 mA and W anode) and Si(Li) detector with resolution of 180 eV at 5.9 kV. The X-ray beam was filtered through a Ti filter. The angle of the incident X-ray beam was 16° at the sample surface. The detector was placed perpendicular to the sample surface. The determination of the sensitivity was performed by the fundamental parameter method, which was based on the mathematical relationship derived from the physical properties and characteristics of the elements and the efficiency of the detection system (Pantenburg et al. 1992). A UV-VIS8500II spectrophotometer (Keda, China) was used to measure the P element content of soils in three replicates.

In this study, three kinds of widely used functions, i.e., linear ($Y=a+bX$), logarithmic ($Y=a+b\ln X$), and third-order polynomial ($Y=a+bX+cX^2+dX^3$), were used to

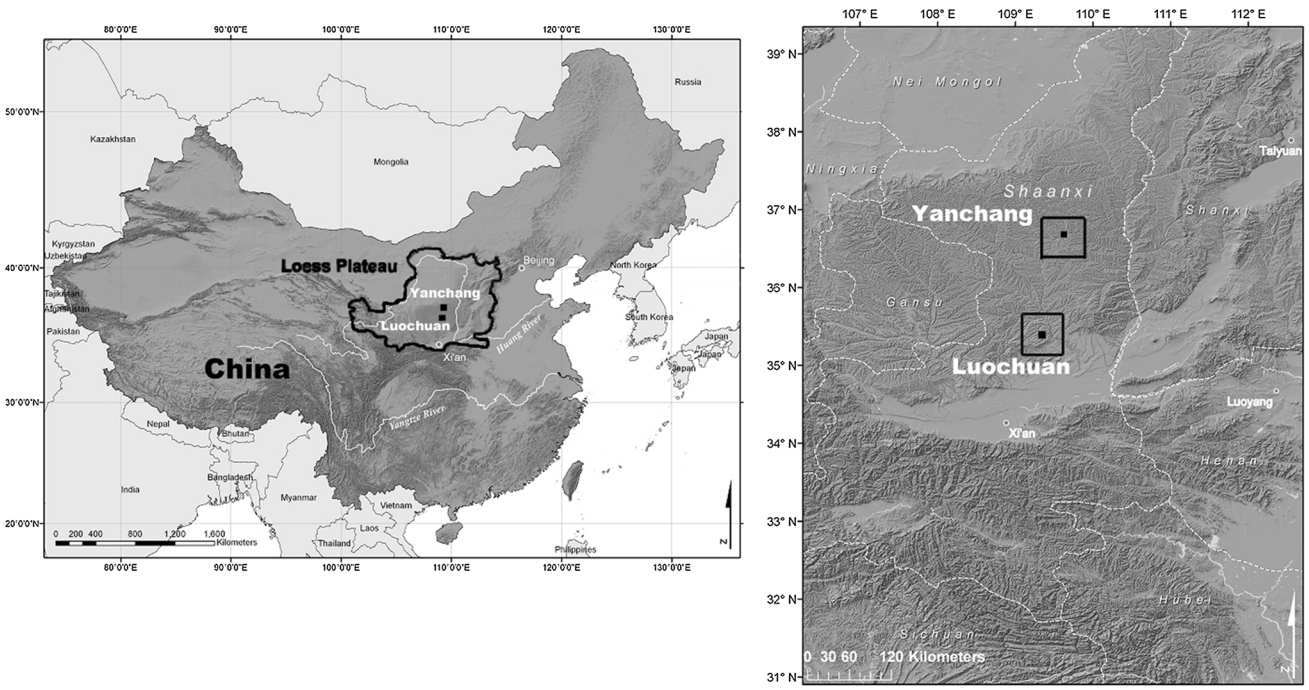

Fig. 1 Location of two soil chronosequences PLC and PYC in Luochuan and Yanchang within the study area on the central Loess Plateau of China

establish the chronofunctions of the dark loessial soil (Bockheim 1980; Schaetzl et al. 1994). The coefficients of determination (r^2) were compared to select the optimal chronofunction. The leave-one-out cross-validation method was employed to calculate the root mean square error of cross-validation (RMSE) and the normalized root mean square error of cross-validation (NRMSE), which were then used to evaluate the models. Statistical and regression analyses were performed using Microsoft Excel 2010 (Microsoft, Redmond, WA, USA), SPSS 19.0 (IBM, Armonk, NY, USA), and Matlab 7.0 (Mathworks, Natick, MA, USA).

Results and discussion

Characteristics of the soil profiles and soil ages

The stratigraphic features and soil horizon designations in the loess-paleosol sequences are described in Table 1. Both the stratigraphic subdivisions and soil horizons were readily identifiable based on comparisons of color, texture, and structure in both the PLC and PYC profiles. The Holocene sequences were on top of the Malan Loess (L_1) layer of the last glaciation in both profiles. The presently ploughed topsoil (TS) was the upper part of the recent loess (L_0). Calcium carbonate concretions (ca. 0.5–1 cm in diameter) were visible below the paleosol (S_0). The soil, exhibiting color heterogeneity and having a smooth boundary (S_0), was buried by the recent loess (L_0). As shown in Table 1, the PLC and PYC profiles both had a layer of dark loessial soil (Ah) beneath their arable layer (Ap). The dark loessial soil is a soil type unique in the classification system of soils in China. It developed on Malan Loess parent material on the Loess Plateau under semi-arid, semi-humid climate conditions, beneath grassland or forest-steppe vegetation. After pedogenic processes occurred over a long period of time, this zonal soil became a type of the main arable soil in the Loess Plateau region (Zhu et al. 1983). Due to severe soil erosion, dark loessial soils have a limited distribution over the central Loess Plateau, and currently exist only on the slightly eroded plateau surface, as well as at the top of ridges and slopes, flat areas in the gully heads, and tablelands. Therefore, two studied profiles had been preserved intact, mainly because the study area has not been strongly eroded.

As can be seen from Table 2, the soil ages of PLC and PYC profiles are 841–12,816 ^{14}C yr BP and 469–12,340 ^{14}C yr BP, respectively. The ^{14}C dates obtained in the humin fraction should be considered as the minimum age of the SOM (Pessenda et al. 2001). The results indicate that the two soil profiles were formed during the Holocene. In addition, with increases in soil depth, the soil age was found to increase, which further confirms the continuity and integrity of the two profiles.

Table 1 Stratigraphic features and soil horizon designations of soil profiles in Luochuan (PLC) and Yanchang (PYC) counties on the central Loess Plateau, China

Profile	Soil horizons	Depth (cm)	Stratigraphic subdivisions	Calendar age (yr BP)	Pedological description
PLC	Ap	0–20	Top soil (TS)	1714 ± 21–0	Light grayish brown, 10YR7/6 (moist), clay loam, weak medium granular structure, slightly hard (dry), abundant roots, some carbonate pseudomycelia in small spots, gradual smooth boundary
	Ah	20–50	Recent loess (L_0)	3171 ± 24–1714 ± 21	Darkish brown, 7.5YR3/3 (moist), clay loam, fine subangular blocky structure, hard (dry), abundant roots, some pseudomycelia in root channels, a few krotowinas filled with C-material, smooth boundary
	AB	50–180	Palaeosol (S_0)	9923 ± 35–3171 ± 24	Color heterogeneity, darkish brown blocks in pale brown soils, clay loam, fine subangular blocks break to granules, slightly hard (dry), few roots, plenty of pseudomycelia, smooth boundary
	Bk	180–190	Transitional layer (L_t)	9923 ± 35–10693 ± 34	Very pale brown, 7.5YR5/3 (moist), clay loam, massive, hard (dry), some very fine pores, few pseudomycelia, some lime nodules of 0.5–1 cm in diameter, few roots, clear boundary
	C	190–200	Malan Loess (L_1)	10693 ± 34–12816 ± 40	Yellowish brown, 10YR8/4 (moist), clay loam, blocks break to granules, slightly hard (dry), few roots
PYC	Ap	0–30	Top soil (TS)	1718 ± 25–0	Light grayish brown, 10YR7/6 (moist), loam, weak medium granular structure, slightly hard (dry), abundant roots, some carbonate pseudomycelia in small spots, gradual smooth boundary
	Ah	30–50	Recent loess (L_0)	2968 ± 23–1718 ± 25	Darkish brown, 7.5YR3/3 (moist), clay loam, fine subangular blocky structure, hard (dry), abundant roots, some pseudomycelia in root channels, a few krotowinas filled with C-material, smooth boundary
	AB	50–160	Palaeosol (S_0)	9841 ± 43–2968 ± 23	Grayish brown, 10YR6/6 (moist), clay loam, massive, hard (dry), little roots, some pseudomycelia in root channels, a few krotowinas filled with C-material, smooth boundary
	Bk	160–180	Transitional layer (L_t)	11090 ± 38–9841 ± 43	Grayish yellow, 2.5Y7/6 (moist), clay loam, massive, hard (dry), few pseudomycelia, some lime nodules of 0.5-1 cm in diameter, few roots, clear boundary
	C	180–200	Malan Loess (L_1)	12340 ± 35–11090 ± 38	Light yellow, 2.5Y8/6 (moist), clay loam, massive, hard (dry)

Soil particle size distribution

It can be seen from the soil particle size analysis of the PLC and PYC profiles that clay (<0.002 mm), silt (0.002–0.02 mm) and sand (0.02–2 mm) in each layer changed with the age of the soil (Fig. 2). In general, the clay and silt contents were higher in the PLC profile than in the PYC profile, and the sand content was lower in the PLC profile than in the PYC profile. This phenomenon occurred because, although both profiles were located on the central Loess Plateau, the PYC profile was from a higher-latitude region, closer to the sources of sandstorms in northwest China (Liu 1985). Under the actions of the monsoon, coarse particles had a shorter transmission range than finer particles (Liu 1985). As a result, the PYC profiles have a higher level of coarse particles compared with the PLC profile. Note that the loessial soil on the Loess Plateau was accretionary, which developed as the parent material was accumulating (Feng and Wang 2005). Another effect of higher latitudes on soil particle size was due to their lower temperatures and reduced rainfall that resulted in less weathering of the PYC profile compared with the PLC profile (White and Blum 1995); this would also result in lower contents of finer soil particles in the PYC profile.

Linear, logarithmic, and third-order polynomial functions were used to fit the relationships among clay, silt, sand and soil age, and the results are shown in Table 3. A third-order polynomial produced the best fitting results for different soil particle compositions and soil ages, and its coefficient of determination was much greater than those of the linear and logarithmic functions. Furthermore, the results of the leave-one-out validation method also showed that the third-order polynomial had the lowest RMSE and NRMSE values. However, this result was not consistent with those obtained in other studies. Barrett (2001) found that the soil silt content and soil age were linearly related,

Table 2 Soil age of each sampled layer of soil profiles in Luochuan (PLC) and Yanchang (PYC) counties on the central Loess Plateau, China

Profile	Depth (cm)	0–10	10–20	20–30	30–40	40–50	50–60	60–70	70–80	80–90	90–100
PLC	^{14}C yr BP (a)	841 ± 32	1714 ± 21	2275 ± 26	2970 ± 21	3171 ± 24	3686 ± 30	3999 ± 23	4443 ± 31	4901 ± 25	5651 ± 26
PYC	^{14}C yr BP (a)	469 ± 25	1093 ± 21	1718 ± 25	2343 ± 22	2968 ± 23	3593 ± 37	4217 ± 30	4842 ± 28	5467 ± 30	6092 ± 28
Profile	Depth (cm)	100–110	110–120	120–130	130–140	140–150	150–160	160–170	170–180	180–190	190–200
PLC	^{14}C yr BP (a)	6052 ± 30	6284 ± 26	7216 ± 34	6159 ± 27	7899 ± 37	7659 ± 29	8154 ± 30	9923 ± 35	10693 ± 34	12816 ± 40
PYC	^{14}C yr BP (a)	6717 ± 33	7341 ± 36	7966 ± 36	8591 ± 33	9216 ± 35	9841 ± 43	10465 ± 44	11090 ± 38	11715 ± 35	12340 ± 35

The half-life of ^{14}C was taken as 5568 years

while Bockheim (1980) and Merritts et al. (1991) concluded that clay content and soil age exhibited a good logarithmic relationship. This may be due to the fact that clay and silt contents of dark loessial soil (Ah layer) in the profiles of this study were greater than those in the upper and lower soil layers, while the sand content was lower than those in the upper and lower soil layers (see Fig. 2). The increase in clay content in a dark loessial soil is not due to leaching and deposition of the overlying soil, but is a product of soil weathering within the profile. Since they were calcareous soils that contained large amounts of calcium and magnesium before decalcification, the negatively charged silicate clay agglomerated with the calcium and magnesium, and the agglomerated clay did not undergo mechanical leaching (Liu 1985). As noted above, weathering would also lead to a decrease in the silt and sand contents. From both the theoretical and practical aspects, this feature of the dark loessial soil profiles was well reflected by a third-order polynomial. Therefore, it can be used as a chronofunction for the soil particle composition of dark loessial soils on the central Loess Plateau.

Organic carbon, $CaCO_3$ and pH value of soil

As can be seen from Table 4, the coefficients of determination were all high (>0.75) and NRMSE were all low (<18 %) when the organic carbon content and soil age in both profiles were fitted by linear, logarithmic, and third-order polynomial functions. However, for the linear and third-order polynomial functions, the *y*-axis intercepts were less than or equal to 0.60, which did not reflect the actual situation. This is because a vegetation-covered soil profile would have the highest organic matter content in the top layer, and this would decrease rapidly with increases in depth, and the rate of decrease would become less after reaching a certain depth (Chen et al. 2005). Studies have shown that the topsoil of dark loessial soils in this region have an organic carbon content of about 1.0 % (Tang and He 2004), which means that the value of the intercept should be at least greater than 1.0. As a result, by indicating that the organic carbon content of the PLC and PYC topsoils were infinitely close to 1.68 and 1.31, the logarithmic functions were consistent with the field observations, and could be used as the chronofunctions for the organic carbon content of the soil in this region. Also, because PLC is located at lower latitudes than PYC, PLC had better hydrothermal conditions for pedogenesis (White and Blum 1995). Therefore, the fact that the PLC profile had a higher organic carbon content in its topsoil than the PYC profile was also consistent with field observations.

Logarithmic functions were also used to fit the $CaCO_3$ content and soil age of the PLC and PYC profiles, but the resulting *y*-axis intercepts were −51.39 and −11.38,

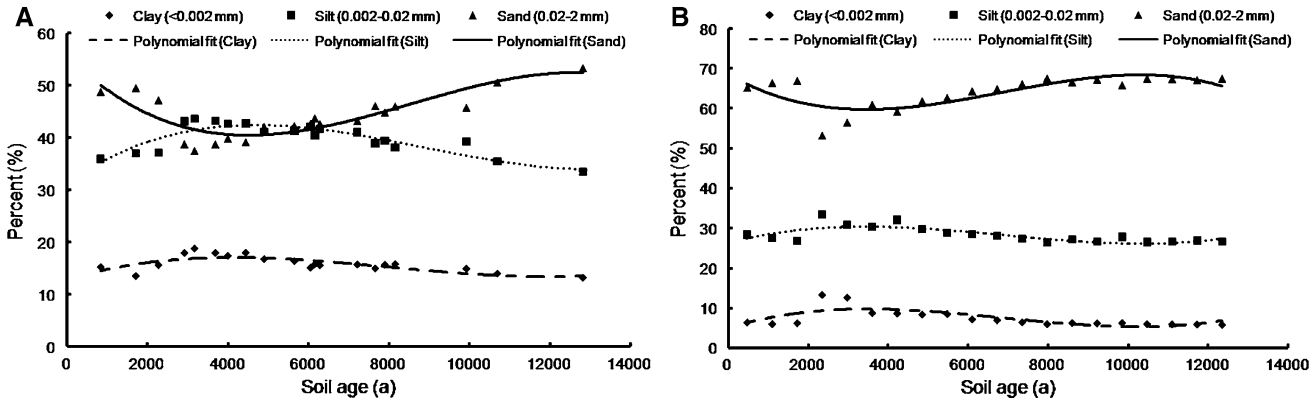

Fig. 2 Different particle-size classification as a function of soil age, with regression curves. **a** The soil profile in Luochuan county (PLC); **b** the soil profile in Yanchang county (PYC)

Table 3 Regression equations for different particle size distributions of the soil profiles in Luochuan (PLC) and Yanchang (PYC) counties on the central Loess Plateau, China

Equations	Profile	Classification	a	b	c	d	r^2	RMSE	NRMSE (%)
$Y = a + bX$	PLC	Clay*	17.39	-2×10^{-4}	–	–	0.26	1.48	26.20
		Silt	42.05	-4×10^{-4}	–	–	0.16	3.11	30.60
		Sand*	40.57	6×10^{-4}	–	–	0.20	4.42	27.95
	PYC	Clay*	9.30	-3×10^{-4}	–	–	0.25	2.08	27.69
		Silt*	30.30	-3×10^{-4}	–	–	0.33	1.79	25.77
		Sand*	60.40	6×10^{-4}	–	–	0.30	3.75	26.21
$Y = a + b \ln X$	PLC	Clay	21.20	−0.62	–	–	0.07	1.71	30.25
		Silt	42.86	−0.35	–	–	0.01	3.47	34.15
		Sand	35.95	0.97	–	–	0.02	5.04	31.85
	PYC	Clay	13.55	−0.72	–	–	0.08	2.38	31.65
		Silt	35.66	−0.86	–	–	0.14	2.07	29.84
		Sand	50.80	1.58	–	–	0.12	4.34	30.31
$Y = a + bX + cX^2 + dX^3$	PLC	Clay**	12.88	24×10^{-4}	-4×10^{-7}	2×10^{-11}	0.59	1.23	21.78
		Silt**	31.38	53×10^{-4}	-8×10^{-7}	3×10^{-11}	0.79	1.97	19.41
		Sand**	55.74	77×10^{-4}	1×10^{-6}	-5×10^{-11}	0.75	3.32	20.97
	PYC	Clay**	4.99	3×10^{-3}	-6×10^{-7}	3×10^{-11}	0.53	1.77	23.62
		Silt**	26.35	27×10^{-4}	-5×10^{-7}	3×10^{-11}	0.61	1.53	22.06
		Sand**	68.66	-58×10^{-4}	1×10^{-6}	-5×10^{-11}	0.60	3.11	21.73

r^2 is the coefficients of determination, *RMSE* root mean square error of cross-validation, *NRMSE* normalized root mean square error of cross-validation

* Level of significance is 0.05, ** Level of significance is 0.01

respectively (Table 4). However, the value of $CaCO_3$ content in a soil cannot be negative, so the function does not show the actual variations of $CaCO_3$ content in the soil. Furthermore, using linear functions to fit the $CaCO_3$ content and soil age of the PLC profile also resulted in a negative y-axis intercept (−2.87). In the fitted results of the PYC profile using a linear function, although the y-axis intercept was positive (7.52), the coefficient of determination was only 0.44 and the NRMSE was only 23.93 %. This indicated that a linear function also cannot describe the relationship between $CaCO_3$ content and soil age. Instead, we found that third-order polynomials could best fit the $CaCO_3$ content and soil age of both the PLC and PYC profiles with coefficients of determination of 0.85 and 0.76, and NRMSE values of 18.37 and 18.96 %, respectively. The resulting curve reflected the fact that topsoil leaching results in deposition of $CaCO_3$ in lower layers, and that the lowest $CaCO_3$ content was found in the dark loessial soil (Ah layer) (see Fig. 3). This result was consistent with the findings of Tang and He (2004) and with those of Zhao et al.

Table 4 Regression equations for the content of organic carbon, $CaCO_3$ and pH value of soil profiles in Luochuan (PLC) and Yanchang (PYC) counties on the central Loess Plateau, China

Equations	Profile	Property	a	b	c	d	r^2	RMSE	NRMSE (%)
$Y = a + bX$	PLC	Organic carbon**	0.57	-3×10^{-5}	–	–	0.79	0.06	12.76
		$CaCO_3$**	−2.87	16×10^{-4}	–	–	0.74	3.24	22.55
		pH value**	8.10	2×10^{-5}	–	–	0.80	0.03	12.00
	PYC	Organic carbon**	0.43	-3×10^{-5}	–	–	0.75	0.06	16.78
		$CaCO_3$**	7.52	6×10^{-4}	–	–	0.44	2.57	23.93
		pH value**	8.60	1×10^{-5}	–	–	0.87	0.02	12.50
$Y = a + b \ln X$	PLC	Organic carbon**	1.68	−0.15	–	–	0.79	0.06	12.18
		$CaCO_3$**	−51.39	6.83	–	–	0.59	4.51	31.35
		pH value**	7.48	0.09	–	–	0.90	0.02	7.75
	PYC	Organic carbon**	1.31	−0.12	–	–	0.98	0.03	9.76
		$CaCO_3$**	−11.38	2.65	–	–	0.53	2.46	22.90
		pH value**	8.23	0.05	–	–	0.92	0.02	9.78
$Y = a + bX + cX^2 + dX^3$	PLC	Organic carbon**	0.60	-5×10^{-5}	8×10^{-10}	2×10^{-14}	0.81	0.08	17.11
		$CaCO_3$**	4.78	-41×10^{-4}	1×10^{-6}	-5×10^{-11}	0.85	2.64	18.37
		pH value**	8.02	6×10^{-5}	-7×10^{-9}	3×10^{-13}	0.88	0.04	14.32
	PYC	Organic carbon**	0.57	-9×10^{-5}	6×10^{-9}	-8×10^{-14}	0.98	0.04	10.82
		$CaCO_3$**	5.48	7×10^{-4}	2×10^{-7}	-2×10^{-11}	0.76	2.04	18.96
		pH value**	8.58	2×10^{-5}	-1×10^{-9}	3×10^{-15}	0.93	0.02	10.64

r^2 is the coefficients of determination, *RMSE* root mean square error of cross-validation, *NRMSE* normalized root mean square error of cross-validation

** Level of significance is 0.01

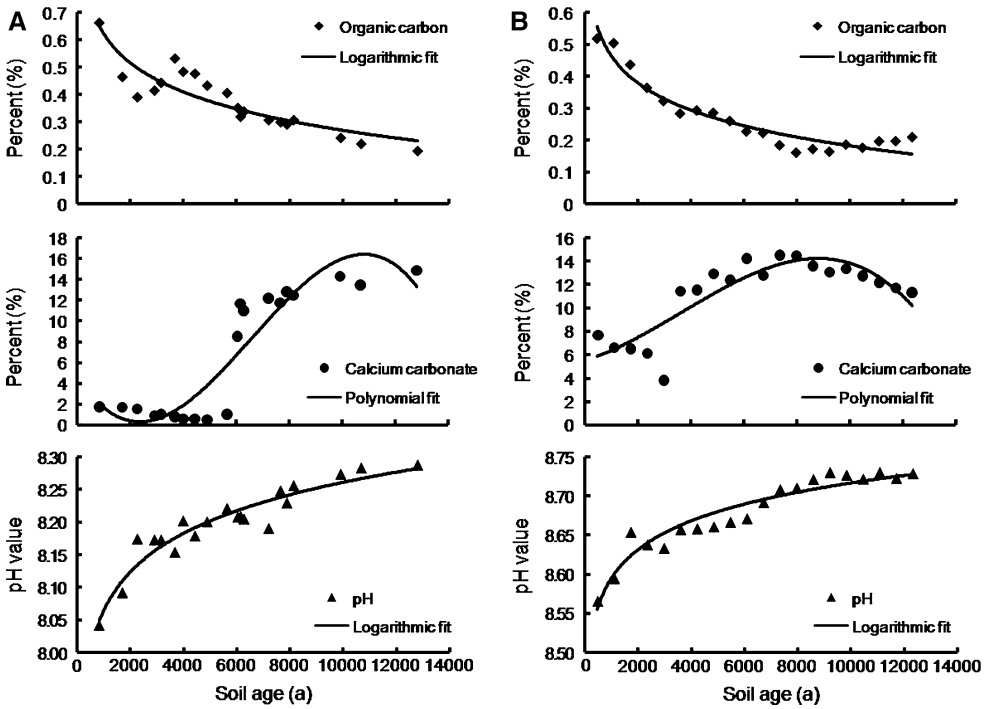

Fig. 3 The content of soil organic carbon, $CaCO_3$ and pH value as a function of soil age, with regression curves. **a** The soil profile in Luochuan county (PLC); **b** the soil profile in Yanchang county (PYC)

(2006) and was in agreement with theoretical predictions and field observations. In addition, due to the lower latitude and greater rainfall amounts at the location of the PLC profile compared with those of the PYC profile, the soil was exposed to more leaching from the upper layers and depositions in the lower layers (see Fig. 3).

Table 5 Regression equations for the ratio of different soil elements and zirconium in the soil profiles in Luochuan (PLC) and Yanchang (PYC) counties on the central Loess Plateau, China

Equations		Ratio	a	b	c	d	r^2	RMSE	NRMSE (%)
$Y = a + bX$	PLC	Fe/Zr**	10362.00	0.22	–	–	0.44	803.20	22.50
		K/Zr**	6175.20	0.15	–	–	0.68	354.46	17.38
		P/Zr**	141.63	0.01	–	–	0.68	24.41	19.48
		Na/Zr**	4092.90	0.10	–	–	0.62	280.23	19.86
		Mg/Zr**	3527.00	0.27	–	–	0.92	295.70	10.84
	PYC	Fe/Zr**	9350.40	0.23	–	–	0.52	914.25	16.45
		K/Zr**	5850.10	0.22	–	–	0.66	666.32	14.39
		P/Zr	204.74	16×10^{-4}	–	–	0.10	19.23	24.64
		Na/Zr**	4304.80	0.15	–	–	0.62	474.22	15.73
		Mg/Zr**	4001.60	0.27	–	–	0.94	284.90	7.38
$Y = a + b \ln X$	PLC	Fe/Zr**	809.08	1276.10	–	–	0.67	740.01	20.73
		K/Zr**	660.09	751.88	–	–	0.78	296.75	14.55
		P/Zr**	−181.56	44.99	–	–	0.61	29.75	23.74
		Na/Zr**	1358.60	392.23	–	–	0.41	384.79	27.27
		Mg/Zr**	−5071.10	1197.70	–	–	0.82	506.01	18.55
	PYC	Fe/Zr**	2105.40	1024.40	–	–	0.57	996.25	17.93
		K/Zr**	208.99	832.07	–	–	0.51	779.44	16.83
		P/Zr**	173.38	4.86	–	–	0.05	19.27	24.70
		Na/Zr**	287.00	585.12	–	–	0.53	523.80	17.37
		Mg/Zr**	−2975.30	1023.80	–	–	0.75	614.88	23.43
$Y = a + bX + cX^2 + dX^3$	PLC	Fe/Zr**	7664.10	1.65	-2×10^{-4}	7×10^{-9}	0.78	666.47	18.67
		K/Zr**	5455.40	0.48	-4×10^{-5}	9×10^{-10}	0.81	260.24	12.76
		P/Zr**	165.90	0.02	6×10^{-6}	-3×10^{-10}	0.84	20.38	16.26
		Na/Zr**	4894.30	−0.44	9×10^{-5}	-4×10^{-9}	0.79	210.55	14.92
		Mg/Zr**	3811.10	−0.04	7×10^{-5}	-4×10^{-9}	0.96	228.87	8.39
	PYC	Fe/Zr**	7138.10	2.20	-4×10^{-4}	2×10^{-8}	0.92	412.18	7.42
		K/Zr**	5409.40	0.93	-2×10^{-4}	1×10^{-8}	0.91	398.59	8.61
		P/Zr**	190.79	0.02	-5×10^{-6}	3×10^{-10}	0.78	10.30	13.20
		Na/Zr**	4037.40	0.48	-7×10^{-5}	4×10^{-9}	0.69	459.24	15.23
		Mg/Zr**	3885.20	0.54	-7×10^{-5}	4×10^{-9}	0.99	136.13	5.19

r^2 is the coefficients of determination, *RMSE* root mean square error of cross-validation, *NRMSE* normalized root mean square error of cross-validation

** Level of significance is 0.01

All three functions also had relatively high coefficients of determination for the fitted relationships between soil pH value and soil age, but the logarithmic function yielded the best fit with a coefficient that was greater than 0.90 and an NRMSE that was lower than 10 %. In addition, the logarithmic function curve best reflected the theories of soil development (see Fig. 3). In the initial stage of soil formation, the alkalization effect of the leaching action occurred relatively quickly in the soil profile (Liu 1985), so that the pH value increased more rapidly in the topsoil, while the rate of increase was less in the lower soil layers. These results were similar to the findings of previous studies (Huang and Gong 2001; Jia et al. 2004).

Migration of chemical elements in soil

The ratio of soil elements that migrate readily to those that seldom migrate, such as Ti or Zr, is often used to study soil enrichment and leaching over time (Egli and Fitze 2000). However, some studies have shown that Ti is also able to migrate, while Zr is less likely to do so (Langley-Turnbaugh and Bockheim 1998; Sauer et al. 2007). Therefore, we used the ratios of a variety of soil elements to Zr to study the migration of elements in soils.

As can be seen in Table 5, a third-order polynomial best fitted Fe/Zr, K/Zr, P/Zr, Na/Zr ratios and soil age of the PLC and PYC profiles, resulting in the highest coefficients

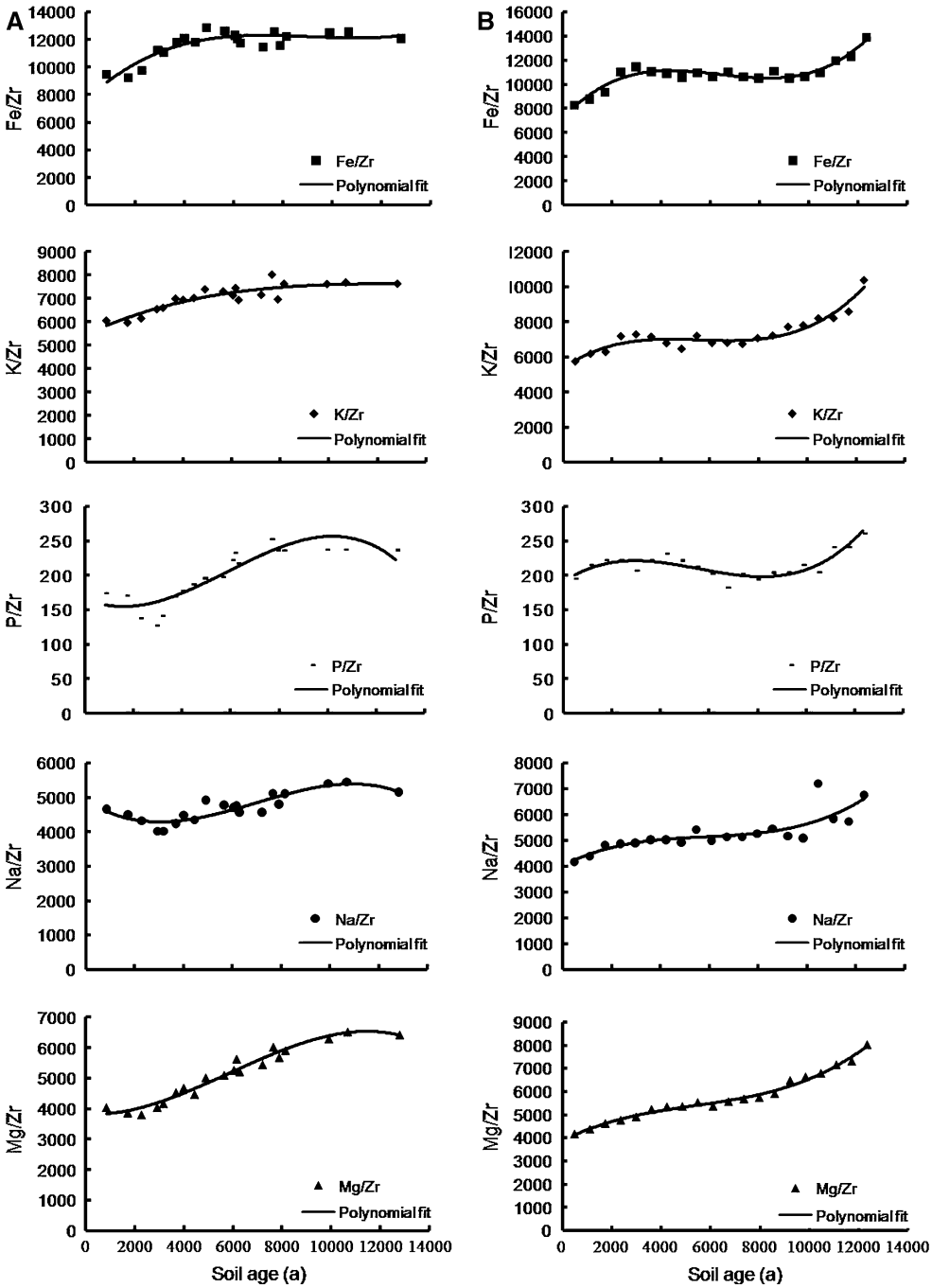

Fig. 4 The ratio of different soil elements and zirconium as a function of soil age, with regression curves. **a** The soil profile in Luochuan county (PLC); **b** the soil profile in Yanchang county (PYC)

of determination and the lowest RMSE and NRMSE values. It could also be seen from Fig. 4 that Fe, K, P and Na in the topsoil were greatly affected by leaching, which was reduced in the lower dark loessial layer and below. The difference between the two profiles was that there was no apparent Fe, K, P and Na enrichment in the older lower layers of the PLC profile, while there was a slight enrichment of these elements in the lower layers of the PYC profile. This may be because the contents of coarser sand increased in the lower layers of the PLC profile (see Fig. 2), resulting in increased permeability that reduced the concentration of the deposited elements in those layers. However, other studies have shown that Fe and K elements in soil have a linear or logarithmic relationship with soil age (Koutaniemi et al. 1988; Lichter 1998; Egli and Fitze 2000; Sauer et al. 2007), which may be related to the soil types and degrees of their development. In contrast, P and Na elements and soil ages still showed linear or logarithmic relationships in non-calcareous soils (Lichter 1998; Egli and Fitze 2000; Sauer et al. 2007).

In addition, it can be seen from Table 5 that third-order polynomial and linear functions yielded very similar coefficients of determination when fitting the Mg/Zr and soil age in both the PLC and PYC profiles, and they also exhibited very similar trends. The difference was that the third-order polynomial suggested that Mg underwent rapid leaching from the topsoil and, with the increase in soil age, the amount of leaching gradually decreased until the content became stable and was equal to that of the parent material (see Fig. 4). In contrast, the linear function indicated that Mg in the soil profiles underwent leaching at a constant rate, which was inconsistent with our field observations.

Conclusions

In this paper, the physical and chemical characteristics, as well as ^{14}C age of Holocene dark loessial soil in Luochuan and Yanchang Counties on the Central Loess Plateau, were studied and fitted using linear, logarithmic, and third-order polynomial functions. The results show that the relationships between the physical and chemical characteristics of the soil and soil age varied in the different soil profiles.

In the PLC and PYC profiles, third-order polynomials yielded the best fits for the relationships of soil clay, silt, and sand contents to soil age. The trend reflected by the third-order polynomial indicated that argillation led to increased clay and silt contents in the dark loessial soil and decreased sand contents. Thus, third-order polynomials were better suited for representing the characteristics of dark loessial soil in the profile.

The age-related variations in organic carbon content and pH values in the soil were best reflected by logarithmic functions. The difference was that the organic carbon content in the soil decreased rapidly with soil age before reaching a certain level, and the decrease rate reduced with age. Meanwhile, the pH value increased rapidly with soil age before reaching a certain level, and the rate of increase reduced with age.

The $CaCO_3$ content and migration of various elements in the soil could best be described by third-order polynomials. However, the trends of the Fe/Zr, K/Zr, P/Zr and Na/Zr ratios were also close to those exhibited by logarithmic function, indicating that Fe, K, P and Na elements in the topsoil were strongly affected by leaching. However, there was no apparent Fe, K, P and Na enrichment in the older lower layers of the PLC profile, while they were slightly enriched in the lower layers of the PYC profile. The third-order polynomial for Mg/Zr showed that Mg underwent strong leaching from the topsoil, and that the effect of leaching was less obvious as soil age increased until a stable content value was attained.

Acknowledgments This research was jointly supported by the National Natural Science Foundation of China (No. 41201270) and Open Research Fund of State Key Laboratory of Simulation and Regulation of Water Cycle in River Basin (China Institute of Water Resources and Hydropower Research) (Grant No. IWHR-SKL-201219). We thank the anonymous reviewers for their helpful comments.

References

Barrett LR (2001) A strand plain soil development sequence in Northern Michigan, USA. Catena 44:163–186

Birkeland PW (1984) Holocene soil chronofunctions, Southern Alps, New Zealand. Geoderma 34:115–134

Bockheim JG (1980) Solution and use of chronofunctions in studying soil development. Geoderma 24:71–84

Chen XY, Wu LG, Li SL, Luo LP (1998) Genesis and evolution of Heilu soils in the south of Wumeng in the Holocene. Chin J Soil Sci 29:241–244 (in Chinese with English abstract)

Chen QQ, Shen CD, Sun YM, Peng SL, Yi WX, Li ZA, Jiang MT (2005) Mechanism of distribution of soil organic matter with depth due to evolution of soil profiles at the Dinghushan Biosphere Reserve. Acta Pedol Sin 42:1–8 (in Chinese with English abstract)

Egli M, Fitze P (2000) Formulation of pedologic mass balance based on immobile elements a revision. Soil Sci 165:437–443

Feng ZD, Wang HB (2005) Pedostratigraphy and carbonate accumulation in the last interglacial pedocomplex of the Chinese Loess Plateau. Soil Sci Soc Am J 69:1094–1102

Finke PA, Hutson JL (2008) Modelling soil genesis in calcareous loess. Geoderma 145:462–479

Hu SX (1994) Genesis and evolution of Heilu soils in the middle and east of Gansu Province. Acta Pedol Sin 31:295–304 (in Chinese with English abstract)

Huang CM, Gong ZT (2001) Quantitative studies on development of tropical soils: a case study in northern Hainan Island. Earth Sci J Chin Univ Geosci 26:314–321

Huggett RJ (1998) Soil chronosequences, soil development, and soil evolution: a critical review. Catena 32:155–172

Jia YF, Pang JL, Huang CC (2004) pH value's measurement and research of its palaeoclimatic meaning in the Holocene loess section. J Shaanxi Norm Univ (Natural Science Edition) 32:102–105 (in Chinese with English abstract)

Koutaniemi L, Koponen R, Rajanen K (1988) Podzolization as studied from terraces of various ages in two river valleys, northern Finland. Silvia Fenn 22:113–133

Langley-Turnbaugh SJ, Bockheim JG (1998) Mass balance of soil evolution on late Quaternary marine terraces in coastal Oregon. Geoderma 84:265–288

Lichter J (1998) Rates of weathering and chemical depletion in soils across a chronosequence of Lake Michigan sand dunes. Geoderma 85:255–282

Liu TS (1985) Loess and arid environment. Science Press, Beijing, pp 191–347 (in Chinese)

Liu G, Liu PL, Yang MY, Cai CF, Xu WN, Zhang Q, Yang W (2013) The significance and relationships among substitutive climatic proxies in the Holocene at the middle Loess Plateau in China. Environ Earth Sci 70:2997–3004

Merritts DJ, Chadwick OA, Hendricks DM (1991) Rates and processes of soil evolution on uplifted marine terraces, northern California. Geoderma 51:241–275

Mook WG, Streurman HJ (1983) Physical and chemical aspects of radiocarbon dating. In: Mook WG, Waterbolk HT (eds) Proceedings of the First International Symposium (=PACT 8). ^{14}C and Archaeology, Strasbourg, p 31–55

Pantenburg FJ, Beier T, Hennrich F, Mommsen H (1992) The fundamental parameter method applied to X-ray fluorescence analysis with synchrotron radiation. Nucl Instrum Methods Phys Res B 68:125–132

Pessenda LCR, Gouveia SEM, Aravena R (2001) Radiocarbon dating of total soil organic matter and humin fraction and its comparison with 14C ages of fossil charcoal. Radiocarbon 43:595–601

Ramsey CB (2001) Development of the radiocarbon calibration program. Radiocarbon 43:355–363

Reimer PJ, Baillie MGL, Bard E, Bayliss A, Beck JW, Bertrand CJH, Blackwell PG, Buck CE, Burr GS, Cutler KB, Damon PE, Edwards RL, Fairbanks RG, Friedrich M, Guilderson TP, Hogg AG, Hughen KA, Kromer B, McCormac G, Manning S, Ramsey BC, Reimer RW, Remmele S, Southon JR, Stuiver M, Talamo S, Taylor FW, Van der Plicht J, Weyhenmeyer CE (2004) IntCal04 terrestrial radiocarbon age calibration, 0–26 cal kyr BP. Radiocarbon 46:1029–1058

Sauer D, Schellmann G, Stahr K (2007) A soil chronosequence in the semi-arid environment of Patagonia (Argentina). Catena 71:382–393

Schaetzl RJ, Barrett LR, Winkler JA (1994) Choosing models for soil chronofunctions and fitting them to data. Eur J Soil Sci 45:219–232

Tang KL, He XB (2002) Revelation on genesis of multi paleosol from Quaternary loess profile. Acta Pedol Sin 39:609–617 (in Chinese with English abstract)

Tang KL, He XB (2004) Re-discussion on loess-paleosol evolution and climatic change on the Loess Plateau during the Holocene. Quat Sci 24:129–139 (in Chinese with English abstract)

Vidic NJ (1998) Soil-age relationships and correlations: comparison of chronosequences in the Ljubljana Basin, Slovenia and USA. Catena 34:113–129

Vincent KR, Bull WB, Chadwick OA (1994) Construction of a soil chronosequence using the thickness of pedogenic carbonate coatings. J Geol Educ 42:316–324

Vogel JS, Southon JR, Nelson DE (1987) Catalyst and binder effects in the use of filamentous graphite for AMS. Nucl Instrum Methods Phys Res B 29:50–56

Vreeken WJ (1975) Principal kinds of chronosequences and their significance in soil history. J Soil Sci 26:378–394

White AF, Blum AE (1995) Effects of climate on chemical-weathering in watersheds. Geochim Cosmochim Acta 59:1729–1747

Wilcke W, Valladarez H, Stoyan R, Yasin S, Valarezo C, Zech W (2003) Soil properties on a chronosequence of landslides in montane rain forest, Ecuador. Catena 53:79–95

Zhao JB, Hao YF, Yue YL (2006) Change of paleosol and climate during middle Holocene in Luochuan area of Shaanxi Province. Quat Sci 26:969–975 (in Chinese with English abstract)

Zhu XM, Li YS, Peng XL, Zhang SG (1983) Soils of the loess region in China. Geoderma 29:237–255